

3D Structural Model of the Bitsmendi Anticline Using Seismic Profiles, Georgia

Victor Alania^{*}, Onise Ehlukidze^{*}, Nino Sadradze^{},
Giorgi Boichenko^{**}, Guga Sadradze^{**}, Alexander Chabukiani^{*},
Tengiz Kiria^{*}, Nino Kvavadze^{*}, Alexander Gventsadze^{*}**

^{*}*M. Nodia Institute of Geophysics, Ivane Javakishvili Tbilisi State University, Tbilisi, Georgia*

^{**}*Institute of Earth Sciences, Ilia State University, Tbilisi, Georgia*

(Presented by Academy Member Tamaz Chelidze)

In this paper, we propose a structural analysis of an active Bitsmendi fold using 2D seismic reflection profiles. The Bitsmendi anticline is located along the frontal part of western Kura foreland fold-and-thrust belt. Our analysis uses subsurface structural geologic techniques to interpret the combination of seismic reflection profiles under the theory of fault-related folding. The interpreted seismic reflection profiles show that the ramp anticline is developed above the location of the main decollement layer and the thrust fault is the main control on the fault-propagation fold forming the Bitsmendi anticline. We identified a strike-slip fault in the eastern segment of Bitsmendi fault-propagation fold. For the interpretation of seismic reflection profiles and construction of a 3D structural model we used Move software. Combining the studies of the structural geometry and previous studies, we infer that the Bitsmendi fault-propagation fold is active and potentially seismogenic. © 2020 Bull. Georg. Natl. Acad. Sci.

Kura foreland basin, seismic reflection profile, fault-propagation fold, 3D structural model

An integrated study of the structure of active folds is crucial in the evaluation of seismic hazards [1]. The Bitsmendi anticline is the main focus of this study and is located along the frontal part of the western Kura foreland fold-and-thrust belt (Figs. 1, 2). The GPS and historical data as well as recent earthquakes and paleoseismic investigation demonstrated an active deformation in the frontal part of the western Kura foreland fold-and-thrust belt [2-7]. Previous research within the study area (Fig. 2) analysed the structure of frontal part of the western Kura foreland fold-and-thrust belt using

borehole data and field investigations [8,9], but the detailed structural architecture still remains unclear. The southern part of Bitsmendi anticline is nearly completely covered by Quaternary sediments and hence its geometry is not yet fully studied (Fig. 2).

In this paper, we employed interpreted 2D seismic reflection profiles across the Bitsmendi anticline in order to constrain the subsurface geometries. Our analysis uses subsurface structural geologic techniques to interpret the combination of seismic reflection profiles under

the theory of fault-related folding [11,12]. In this study, we present 3D structural model of the Bitsmendi anticline. We applied Move software

(Midland Valley Exploration Ltd.) in the interpretation of seismic reflection profiles and 3D structural modelling.

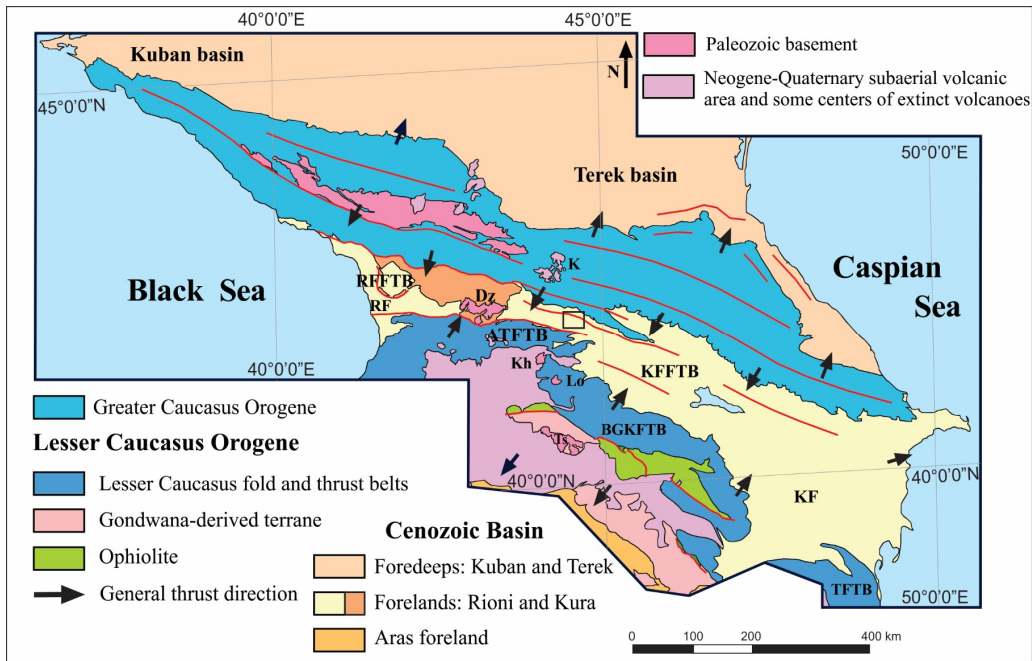


Fig. 1. Tectonic map of the Caucasus [10].

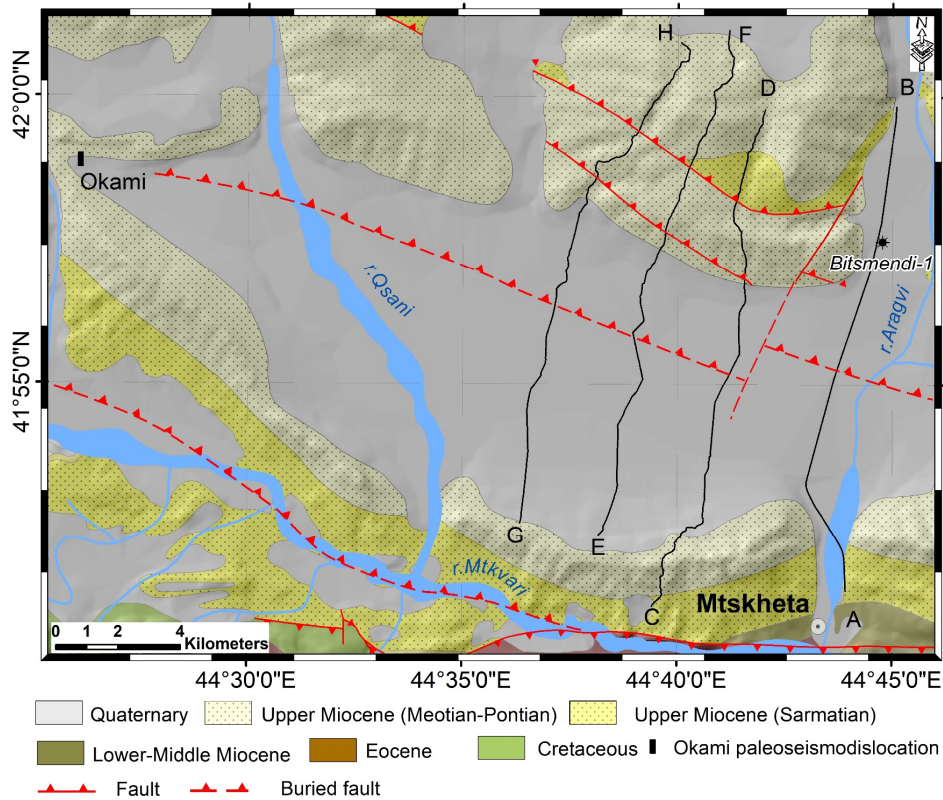


Fig. 2. Geological map of the study area, modified from D. Papava [9].

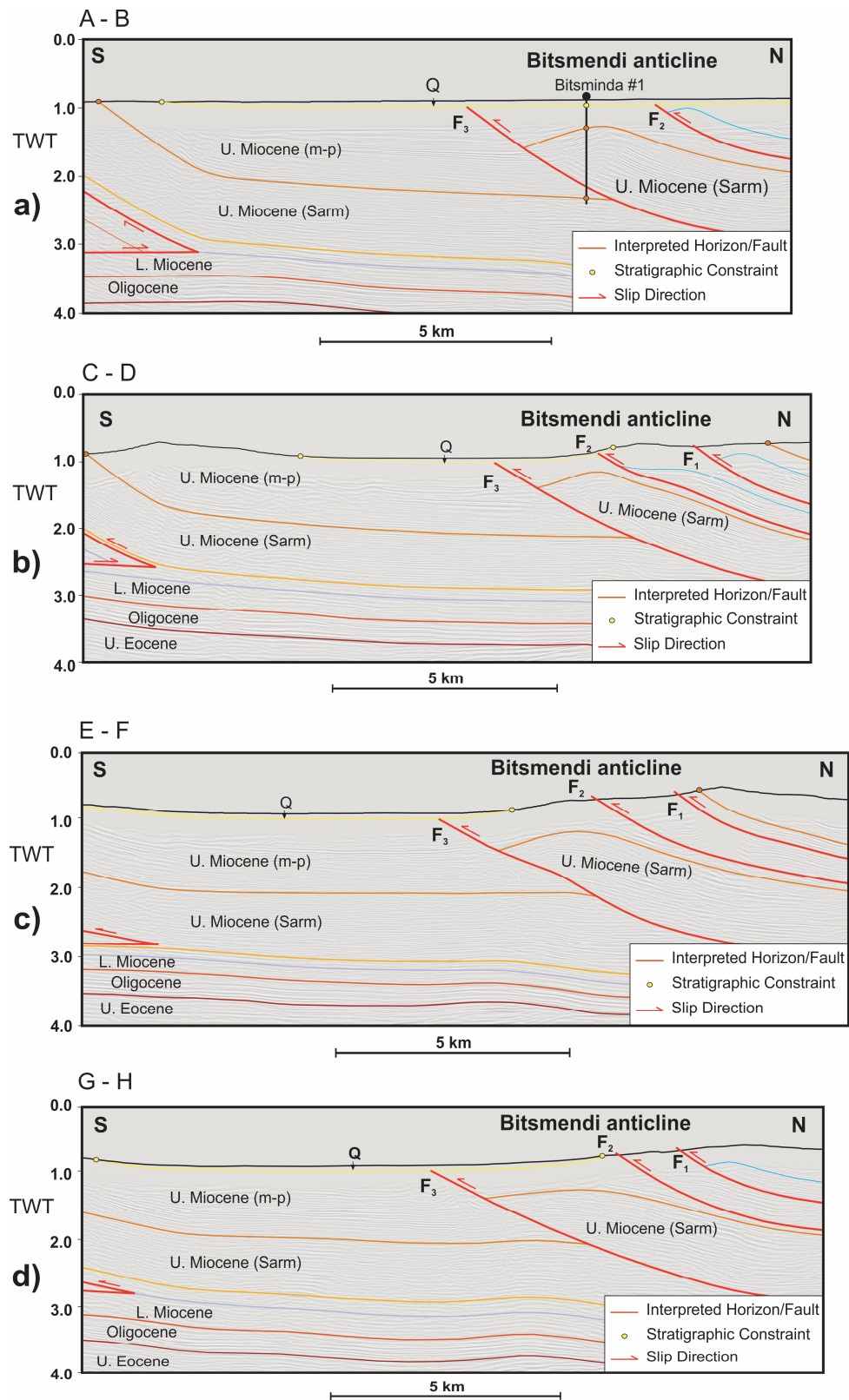


Fig. 3. a) Interpreted seismic profile A-B. b) Interpreted seismic profile C-D. c) Interpreted seismic profile E-F. d) Interpreted seismic profile G-H. Location is shown in Fig. 2.

Geological Setting

Kura foreland thin-skinned fold-and-thrust belt is located between the Lesser and Greater Caucasus orogens (Fig. 1) and is mainly represented by the series of NEN dipping thrust faults, most of which are associated with fault-related folds [8, 13-18]. To the South, the undeformed Kura foreland basin is located between the western Kura foreland fold-and-thrust belt and frontal part of the Lesser Caucasus [8, 16]. Cenozoic continental sediments in the Kura foreland fold-and-thrust belt keep the record on the stratigraphy and structural evolution of the study area during the orogeny [16].

The Kura basin which developed formerly as a foreland basin (Oligocene-Lower Miocene) continued its evolution as a fold-and-thrust belt during Middle Miocene-Pleistocene [16]. The western Kura foreland fold-and-thrust belt contains strata ranging from Oligocene to Quaternary in age and is represented by foreland basin megasequence (Oligocene-Lower Miocene) and syn-tectonic sediments (Middle Miocene-Pleistocene) [16]. Oligocene-Early Miocene sediments in some places conformably follow Late Eocene sandstones [14]. Syn-tectonic deposits are represented by shallow marine (Middle Miocene and lower-middle parts of Upper Miocene) and thick continental (upper part of Upper Miocene – Sarmatian, Meotian-Pontian and Pliocene-Pleistocene) sediments [16]. The Quaternary sediments are mainly unconformably deposited on older layers [14].

Building of south-vergent structures of the western Kura foreland basin was governed by the Greater Caucasus basement wedge(s) propagation along detachment horizons within the cover-generating thin-skinned structures made up of Neogene shallow marine and thick continental sediments [19].

Seismic Interpretation of Bitsmendi Anticline

For understanding of the geometry of the Bitsmendi anticline, we selected four seismic cross-sections (A-B, C-D, E-F, G-H) across the anticline that are based on a post-stack time-migration, which offers clear images of faults and related folds (Fig. 3). The location of the seismic reflection profiles is shown in Fig. 2.

The surface geological information is obtained from 1:50000 geological map (Fig. 2). Identification of stratigraphic units at depth for seismic profiles was based on outcrop data correlations.

The interpreted seismic reflection profiles (A-B, C-D, E-F, G-H) show that the ramp anticline is developed above the location of main decollement layer (the lower part of Sarmatian – upper Miocene). The seismic reflection profile C-D, E-F, G-H revealed the geometry of Bitsmendi anticline. The interpretation results match with the seismic reflection profile A-B (Fig. 3). The final structural model comprises five horizons (i.e., the top of Sarmatian – Upper Miocene, Middle Miocene, Lower Miocene, Oligocene and Upper Eocene), three main south-vergent thrust faults (i.e., F_1 , F_2 , and F_3) and a strike-slip (F_4). The location of F_3 fault (or thrust) has been identified in all seismic reflection profiles (Fig. 2). The backlimb of the fold dips gently (8° – 3°) to the north, whereas the forelimb dips steeply (13° – 11°) to the south, and steepens with increasing depth (Fig. 3). The interpreted seismic reflection profiles (Fig. 3) show that the ramp anticline is developed above the location of the main decollement layer and that the thrust fault (F_3) is the main control on the fault-propagation folding that formed the Bitsmendi anticline. In the backlimb, the lack of any dip planes that are parallel to the underlying fault ramp, suggests that a process of shearing is an important mechanism in the deformation of the Bitsmendi anticline.

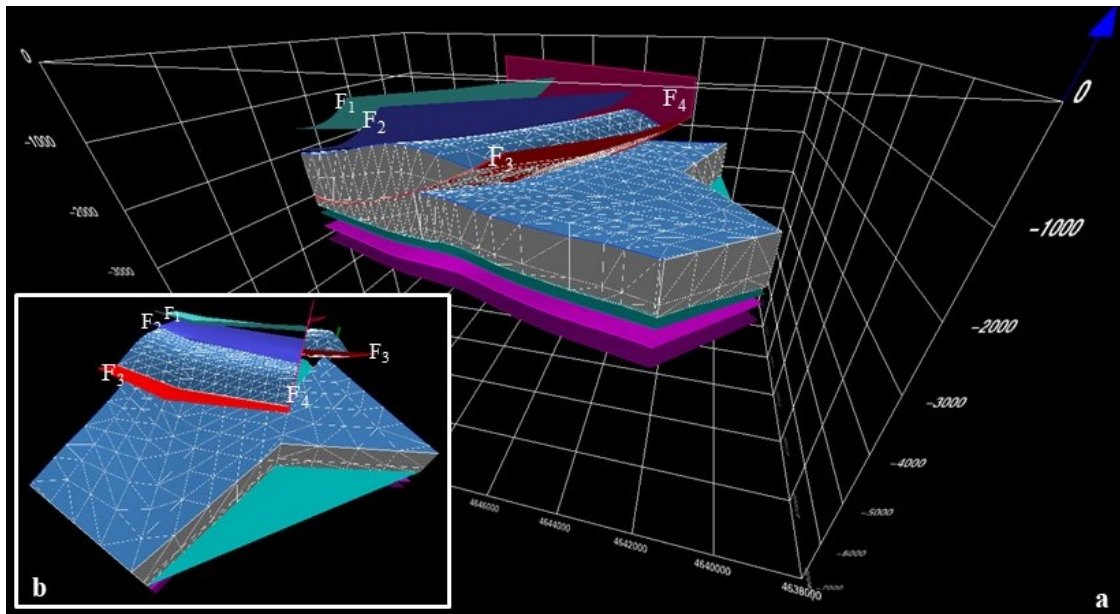


Fig. 4. a) 3D structural model of the Bitsmendi anticline. Perspective view, looking from the West. b) Perspective view, looking from the South.

Discussion

The geometry of folds is the most important because it is a direct fault geometry and is the most commonly available and continuous data set in fold-and-thrust belts and provides information only along the chosen plane of section. In many cases, 3D analysis is vital to constrain subsurface structural geometry [1, 20]. Lateral changes in fold and fault trends often play important part in forming structural traps for hydrocarbons and assessing the hazards posed by active seismogenic faults [21].

We used the 3D models to examine the spatial relationship between the frontal thrust faults and the Bitsmendi anticline and along-strike variations in fault geometry (Fig. 4). The 3D modeling was performed in the following order: (1) structural interpretation of 2D seismic reflection profiles; (2) interpolation of identified horizons, faults and thrusts and their connection. The 3D structural model (Fig. 4) reveals that the F_3 fault comprises a basal detachment and thrust ramp, and the thrust fault serves as the main control on the fault-propagation folding that formed the Bitsmendi

anticline. We believe that paleoseismodislocation (potential coseismic rupture) located near the village Okami [3] should be associated with the western extension of the F_3 fault (Fig. 4).

Conclusion

1. We reveal the deformation style of the Bitsmendi anticline, based on the seismic reflection data, field observations, and 3D structural modelling.
2. We suggest that Bitsmendi anticline is a fault-propagation fold.
3. We identify a strike-slip in the eastern segment of the Bitsmendi fault-propagation fold.
4. Combining the studies of the structural geometry and previous studies we infer that the Bitsmendi fault-propagation fold is active and potentially seismogenic.

The work was supported by Shota Rustaveli National Science Foundation of Georgia (SRNSF #217942- structure, time and magnitude of deformation of the eastern Achara-Trialeti fold and

thrust belt, and SRNSF, #217408. Interactive Geological Map of Georgia, 1:200000 scale). We are thankful to “Midland Valley” for providing the Move program for their Academic Support Initiative Program. We are very grateful to

Georgian State Agency of Oil and Gas and Georgian Oil & Gas Limited for providing the seismic profiles for our seismic interpretation. We would like to thank Prof. Shota Adamia for discussions.

გეოფიზიკა

ბიწმენდის ანტიკლინის სამგანზომილებიანი სტრუქტურული მოდელი სეისმური პროფილების გამოყენებით, საქართველო

ვ. ალანია*, ო. ენუქიძე*, ნ. სადრაძე**, გ. ბოიჩენკო**, გ. სადრაძე**,
ა. ჭაბუკიანი*, თ. ქირია*, ნ. ყვავაძე*, ა. გვენცაძე*

* ივანე ჯავახიშვილის თბილისის სახელმწიფო უნივერსიტეტი, მ. ნოდიას გეოფიზიკის ინსტიტუტი, თბილისი, საქართველო

** ილიას სახელმწიფო უნივერსიტეტი, დედამიწის შემსწავლელი ინსტიტუტი, თბილისი, საქართველო

(წარმოდგენილია აკადემიის წევრის თ. ჭელიძის მიერ)

სტატიაში წარმოდგენილია ბიწმენდის აქტიური ნაოჭის სტრუქტურული ანალიზი, ორგანზომილებიანი არეკვლილი სეისმური პროფილების გამოყენებით. ბიწმენდის ანტიკლინი განლაგებულია დასავლეთ მტკვრის ფორლანდის ნაოჭა-შეცოცებითი სარტყლის ფრონტული ნაწილის გასწვრივ. რღვევებთან დაკავშირებული ნაოჭების თეორიაზე დაყრდნობით სეისმური პროფილების კომბინაციის ინტერპრეტაციის მიზნით ანალიზში გამოყენებულია სტრუქტურული გეოლოგიის სიღრმული კვლევის მეთოდები. ინტერპრეტირებული სეისმური პროფილებიდან ჩანს, რომ რამპანტიკლინი განვითარებულია ძირითადი მოწყვეტის ზედაპირის თავზე, ხოლო შეცოცება წარმოდგენდა ბიწმენდის ანტიკლინის წარმომქმნელი რღვევა-გავრცელებადი დანაოჭების მთავარ მაკონტროლებელ ფაქტორს. ბიწმენდის რღვევა-გავრცელებადი ნაოჭის აღმოსავლეთ სეგმენტში დადგინდა ნაწევი. სეისმური პროფილების ინტერპრეტაციის და სამგანზომილებიანი სტრუქტურული მოდელის აგებისათვის გამოყენებულია კომპიუტერული პროგრამა Move. სტრუქტურული გეომეტრიისა და წინა კვლევების შედეგების გათვალისწინებით ვვარაუდობთ, რომ ბიწმენდის რღვევა-გავრცელებადი ნაოჭი არის აქტიური და პოტენციურად სეისმოგენური.

REFERENCES

1. Tibaldi A., Russo E., Bonali F. L., Alania V., Chabukiani A., Enukidze O., Tsereteli N. (2017) 3-D anatomy of an active fault-propagation fold: a multidisciplinary case study from western Caucasus, Tsaishi (Georgia). *Tectonophysics*, **717**: 253-269.
2. Adamia Sh., Alania V., Tsereteli N., Varazanashvili O., Sadradze N., Lursmanashvili N., Gventsadze A. (2017) Postcollisional tectonics and seismicity of Georgia. *Geological Society of America, Special Papers*, **525**: 535-573.
3. Boichenko G., Cowgill E., Stahl T., Trexler C., Tsiskarishvili L., Sukhishvili L., Sokhadze G. et al. (2016) A paleoseismic investigation of a frontal foreland thrust in the Greater Caucasus, Georgia. *AGU Fall Meeting Abstracts*, 120-121. Denver.
4. Reilinger R. et al. (2006) GPS constraints on continental deformation in the Africa–Arabia–Eurasia continental collision zone and implications for the dynamics of plate interactions. *Journal of Geophysical Research*, **111**: 1-16.
5. Sokhadze G., Floyd M., Godoladze T., King R., Cowgill E. S., Javakhishvili Z., Hahubia G., Reilinger R. (2018) Active convergence between the Lesser and Greater Caucasus in Georgia: constraints on the tectonic evolution of the Lesser–Greater Caucasus continental collision. *Earth and Planetary Science Letters*, **481**: 154–161.
6. Tan O., Taymaz T. (2006) Active tectonic of the Caucasus: earthquake source mechanisms and rupture histories obtained from inversion of teleseismic body waves. *Geological Society of America, Special Paper*, **409**: 531–578.
7. Tsereteli N., Tibaldi A., Alania V., Gventsadze A., Enukidze O., Varazanashvili O., Müller B. I. R. (2016) Active tectonics of central-western Caucasus, Georgia. *Tectonophysics*, **691**: 328–344.
8. Banks C. J., Robinson A. G., Williams M. P. (1997) Structure and regional tectonics of the Achara-Trialet fold-belt and the adjacent Rioni and Karli foreland basins, Republic of Georgia. *Regional and Petroleum Geology of the Black Sea and Surrounding Region*, 331–346.
9. Papava D. (1967) Voprosy geologii vostochnoi chasti Trialetskogo khrebtia i perspektivy neftegazonosnosti melovykh i paleogenovykh otlozhenii, 188-204 Leningrad (in Russian).
10. Alania V., Enukidze O., Giorgadze A., Glonti N., Glonti B., Koiava K., Razmadze A. et al. (2018) Structural architecture of the Kura foreland fold-and-thrust belt using seismic reflection profile, Georgia. *Universal Journal of Geoscience*, **6**: 184-190.
11. Shaw J. H., Connors C. D., Suppe J. (2006) Seismic interpretation of contractional fault-related folds. *AAPG Studies in Geology*, **53**: 156.
12. Suppe J., Medwedeff D. A. (1990) Geometry and kinematics of fault-propagation folding. *Eclogae Geologicae Helveticae*, **83**: 409–454.
13. Adamia Sh., Alania V., Ananiashvili G., Bombolakis E., Chichua G., Girshiashvili D., Martin R., Tatarashvili L. (2002) Late Mesozoic-Cenozoic geodynamic evolution of the eastern Georgian oil-gas bearing basins. *Geologica Carpathica*, **53**: 155-159.
14. Adamia Sh., Alania V., Chabukiani A., Chichua G., Enukidze O., Sadradze N. (2010) Evolution of the Late Cenozoic basins of Georgia (SW Caucasus): a review. *Geological Society, London, Special Publication*, **340**: 239-259.
15. Alania V., Enukidze O., Koiava K., Razmadze A., Sanishvili A. (2008) Thrust systems and time of deformation of the Gare Kakheti foothills, eastern Georgia (Georgia). *Bollettino di Geofisica, teorica ed applicate*, **49**: 207-208.
16. Alania V., Chabukiani A., Chagelishvili R., Enukidze O., Gogrichiani K., Razmadze A., Tsereteli N. (2017) Growth structures, piggyback basins and growth strata of Georgian part of Kura foreland fold and thrust belt: implication for Late Alpine kinematic evolution. *Geological Society, London, Special Publications*, **428**: 171-185.
17. Forte A., Cowgill E., Bernardin T., Kreylos O., Hamann B. (2010) Late Cenozoic deformation of Kura fold-thrust belt, southern Greater Caucasus. *Geological Society of America Bulletin*, **122**: 465–486.
18. Sosson M., Stephenson S., Adamia Sh., Avagyan A., Kangarli K., Starostenko V., Yegorova T., Sheremet Y., Barrier E., et al. (2016) The Eastern Black Sea-Caucasus region during Cretaceous: new evidence to constrain its tectonic evolution. *Compte-Rendus Geosciences*, **348** (1): 23-32.
19. Alania V. et al. (2018) Structural geometry of active Kura foreland fold-and-thrust belt revealed by seismic reflection profiles. EGU General Assembly 2018. *Geophysical Research Abstracts*, **20**: EGU2018-9864.
20. Li Y., Jia D., Shaw J., Hubbard J., Lin A., Wang M., Luo L., Li H., Wu L. (2010) Structural interpretation of the coseismic faults of the Wenchuan earthquake: Three-dimensional modeling of the Longmen Shan fold-and-thrust belt. *Journal of Geophysical Research*, **115**: 1-26.
21. Shaw J. H., Hook S. C., Suppe J. (1994) Structural trend analysis by axial surface mapping: *AAPG Bulletin*, **78**: 700–721.

Received July, 2019